Comparing COVID-19 lockdown strategies with a stochastic cellular automaton

Spencer Passmore

14 November 2021

Contents

1 Summary

We propose a stochastic cellular automata model for epidemics that draws from the principles behind the SEIR model, and groups cells into separate "regions". Each cell can contain any number of individuals, and each region is a square grid of cells of varied size. This regional model is shown to be able to accurately replicate historical disease data of an isolated society (specifically, the Faroe Islands). We use the model to compare lockdown approaches in the context of Covid-19 in metropolitan Melbourne, Australia. Specifically, we compare imposing restrictions in all regions, and only restricting regions where cases have been detected. We find a significant increase in disease spread when the latter approach is used for a range of parameters.

2 Introduction

2.1 How the Abelian Sandpile Model relates to epidemics.

The Bak-Tang-Wiesenfeld model, or the sandpile model, is the canonical example of self-organised criticality (SOC) (Per Bak, Tang, and Wiesenfeld 1987). In it, we consider a square grid of cells that can contain up to, for example, 3 grains of sand. At 4 grains of sand (the critical parameter), the stack topples, depositing one grain of sand on each directly adjacent cell. Grains of sand can be dropped randomly, or on one cell repeatedly – in the latter case, fractal structures emerge, only varying in detail with larger grid size (Pegden and C. K. Smart 2020).

The sandpile model, as with all SOC systems, demonstrates emergence and self-organisation, in that complex but ordered behaviours arise from an initially disordered state (P. Bak and Paczuski 1995). A change to a single part of the system leads to a change in any number of parts of the system, as a toppling can trigger from none to countless other topplings. This is known as "critical behaviour", and mirrors real-world phenomena such as forest fires and avalanches. Of great interest, SOC systems all follow their own critical behaviours for a wide range of parameters, which might explain their prominence in emergent phenomena in nature.

The fractal nature of the sandpile model, or its scale-invariance, is shared with all SOC systems, and this is due to the statistical properties of the system being governed by power laws (Golyk 2012). Such power laws can usually be identified by considering the distributions of the sizes of the cascades of activity in the systems (such as the number of sites in the sandpile model that topple at once). It has been shown that epidemics in isolated populations seem to demonstrate SOC in that, up to a point, their distributions in number of people infected obey such power laws (Rhodes, Jensen, and Anderson 1997). This power law is the following:

$$n(s) \propto s^{-\kappa} \tag{1}$$

Where $n(s)$ is the frequency of epidemics, s is the number of individuals infected (the size of the "cascade"), and κ is the scaling exponent, which varies between diseases. The historical data for the Faroe Islands shows the islands obeying this power law up until the point where epidemics are of a size of around 1000 cases, where the number of larger-sized events falls off rapidly (the population of the islands being approximately 25,000). This arises due to the "boundary" of the system (no more than 25,000 people can be infected), and is similar to how the sandpile model's cascades obeys power law up until cascades larger than half the number of cells in the square grid (Kalinin et al. 2018).

So how do we model this SOC? The standard forest-fire model is another standard SOC cellular automaton introduced not long after the sandpile model, and is easily generalisable to disease. In this model, a grid of cells can either hold a tree, hold a burning tree, or be empty. The standard rules that the model followed were that after each time-step, all cells with trees adjacent to burning trees becoming cells with burning trees themselves. If we implement a rate of tree regrowth (b), and a chance

for trees to spontaneously combust f, we can see disease-like behaviour. (So long as $T \ll b^{-1} \ll f^{-1}$, where T is the time taken for a cluster of trees of order of the number of cells on the grid to burn down.) If we instead consider trees to be individuals, burning trees to be infected individuals, and empty cells to be immune (or deceased) individuals, then b is the rate of births, and f^{-1} gives us the timescale over which epidemics occur.

Increasing the dimension of the model is equivalent to reducing the effective reproduction rate of the disease (Rhodes, Jensen, and Anderson 1997). However, in adapting this model into a more nuanced one for epidemics, we will aim to approximate the exponent only through modifying the effective reproduction rate of the disease, staying within 2 dimensions. The benefit of this is the model remains a geographical space, which allows for easy visualisation of how diseases spread under varying rates of transmissibility.

2.2 COVID-19 and region-specific disease control

The COVID-19 pandemic has led to a great debate on and interest in the best way societies can respond to pandemics. While without access to vaccines, a common strategy used to control outbreaks has been the implementation of lockdowns. By decreasing the number of contacts individuals have, lockdowns lower the effective reproduction number of the virus (R_e); this reduces stress on health systems by slowing the rate of infection, and lowers the total number of people that will be infected (since R_e will fall below 1 sooner). Even without lockdowns, some societies like South Korea achieved similar results through high rates of compliance to health advice (Kang et al. 2020).

A common aspect of restrictions is that responses such as lockdowns and health mandates have varied between regions of societies, whether due to political differences, or strategies that treat regions separately. In Australia during 2021, the states of New South Wales and Victoria both saw outbreaks of the COVID-19 delta variant, during which lockdowns were implemented. Victoria opted to only distinguish between metropolitan Melbourne and rural Victoria when implementing restrictions for their outbreaks (a "blanket" approach). New South Wales, in their July 2021 outbreak of the delta variant of COVID-19, distinguished restrictions on a local government area (LGA) level, expanding the lockdown area on a much finer level as the outbreak progressed ("reactive"). In both Victoria and New South Wales, regions would be locked down in response to cases being detected in them. By the end of 2021, usually only a day or two of cases prompted this response in both states.

We have constructed a stochastic algorithm that utilises the ideas behind the kind of cellular automata that lead to SOC. We believe this allows us to extend the forest-fire model to simulate disease outbreaks when different spatial groups of cells behave differently. After an overview of the model and the ideas behind it, we will show that this model is able to accurately simulate the spread of disease in isolated populations like the Faroe Islands. Then, we will extend this model to a mapping of Melbourne, Australia, to compare reactive lockdowns to blanket ones.

3 2. Modelling

3.1 Modelling Outbreaks with Cellular Automatons

The spread of disease among isolated societies has long been known to exhibit the self-organised criticality (SOC) and hence scale invariance of simple cellular automatons (Rhodes, Jensen, and Anderson 1997). Specifically, the forest-fire model is easily generalised to a model of epidemics. In such a model, f^{-1}, the inverse of the frequency of epidemics, is the timescale over which the model has cycles. This timescale must be larger than the time for the epidemic to conclude, which in turn must be larger than the time it takes for cells to infect one another.

In the context of comparing the effectiveness of strategies in defending against an unprecedented disease like COVID-19, we only wish to consider the timescale of a single epidemic. There is no guarantee that

using the model above would represent an "average" of what we would expect in the real world. In real life, random chance dominates when case numbers are low, potentially leading to a significant variance in results such as the length of the epidemic. While normally the cycles of SOC provide insight into the cyclic nature of phenomena (such as the frequency of burnings or outbreaks), this cannot occur due to our timescale being lower than f^{-1}.

Extending cellular automata to stochastic cellular automata has shown success in qualitatively analysing such time scales. For example, extending the forest-fire model to a stochastic one will produce different burning patterns, and averaging them out produces a map of the likelihood of a given cell to burn (Almeida and Macau 2011).

3.2 Modelling Outbreaks with Compartmental Models

It is generally unrealistic to run simulations of millions of cells interacting with each other. As such, computational models of COVID-19 have often been based on the idea of "compartmental models". The simplest of these being the Susceptible-Infected-Recovered (SIR) model. This model takes the form of a system of ODEs:

$$\frac{dS}{dt} = \frac{-\mu R_0 I S}{N} \tag{2}$$

$$\frac{dI}{dt} = \mu \left(\frac{R_0 I S}{N} - I \right) \tag{3}$$

$$\frac{dR}{dt} = \mu I \tag{4}$$

where S, I, and R are the number of susceptible, infected, and recovered individuals respectively; R_0 is the basic reproduction number, N is the size of the population, and μ^{-1} is the average time for an individual to recover.

This model is deterministic, and it assumes that the length of time required for individuals to transition from the infected to the recovered state is exponential. Additionally, as with SOC, it is scale invariant.

Simple compartmental models depend only on the number of individuals in each category (due to the mass-action assumption). As such, they break down when large numbers of cases are present and are not distributed homogeneously, and this is likely why Monte Carlo simulations that utilise them fail to simulate epidemics in the Faroe Islands (Rhodes, Jensen, and Anderson 1997). For example, consider a country with ten thousand infected individuals. Contrary to Equation (3), we should expect a significant difference in infection rates if these individuals make up most of a small community than if they were spread out around the country, as the local saturation of cases would be far higher than the national saturation. Indeed, the SIR model has been shown to perform poorly in modelling COVID-19, but can be remedied by incorporating spatial components into the model (Kolokolnikov and Iron 2021).

Including this spatial component is especially important given we are primarily interested in the region-based way that contemporary societies respond to pandemics.

3.3 Model Description

The model we use is an inhomogeneous stochastic cellular automaton, that utilises the ideas behind the Susceptible-Exposed-Infected-Recovered (SEIR) compartmental model. The simulation space of this model is made up of connected regions, where a region is a square lattice of cells.

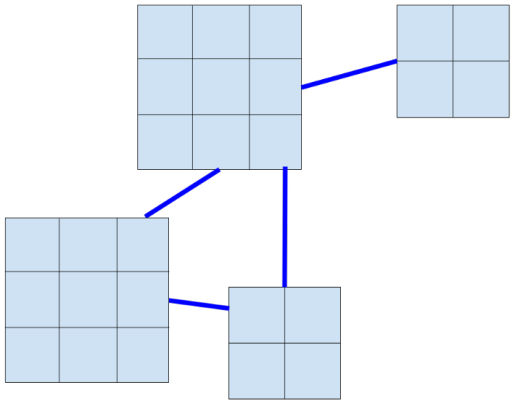

Figure 1: Example of how four regions, two with 9 cells and two with 4 cells, might be connected.

3.3.1 Cell rules

Each cell obeys the following rules:

- The cell has a position (x,y) within a region.
- A cell has any number of individuals that can be in one of five states: susceptible (S), exposed/incubating (E), infected (I), recovered (R), and deceased (D), and these states update each simulated day.
- Individuals in the E state progress to the I state, and in the I state to the R or D state, after a randomly selected number of days. The former obeys a normal distribution, and for the latter we use a truncated exponential distribution[1]. Whether an individual recovers or passes away is randomly determined based on the death rate of the disease.
- On average the change in individuals in the E state each day is given by:

$$\Delta E = (\frac{N_E}{\frac{T_I}{\omega} + T_E} + \frac{N_I}{T_I + \omega \mathrm{T}_E})R_e - \ \Delta \mathrm{I} \tag{5}$$

  where R_e is the effective reproduction number of the disease, N_E and N_I are the number of individuals in the E and I states respectively, T_E and T_I are the average time spent in the E and I states respectively, and ω is the factor that modifies how likely an individual in the E state is to infect someone compared to in the I state.

  When R_e is constant, each individual exposes on average R_e susceptible individuals to the disease throughout their infection (where an exposure guarantees an infection). The number of individuals infected each day is drawn randomly from a truncated normal error distribution.

- Disease-carrying individuals can expose other individuals within their cell and adjacent (non-diagonal) cells. There is also a relatively small chance that an "interregional contact" can occur, where a disease-carrying individual exposes an individual in a cell randomly chosen from within the current region or connected regions. We designate the ratio of non-interregional contacts and interregional contacts to be r, and this value will depend on the scenario.

[1] Using a normal distribution differs from the standard SEIR model, but we choose it here as incubation times for COVID-19 follow a lognormal distribution (Paul and Lorin 2020), and, for the Melbourne scenario, we do not wish to underestimate the median incubation period. Moving to a lognormal distribution would improve the model and can be implemented in the same way the exponential distribution was.

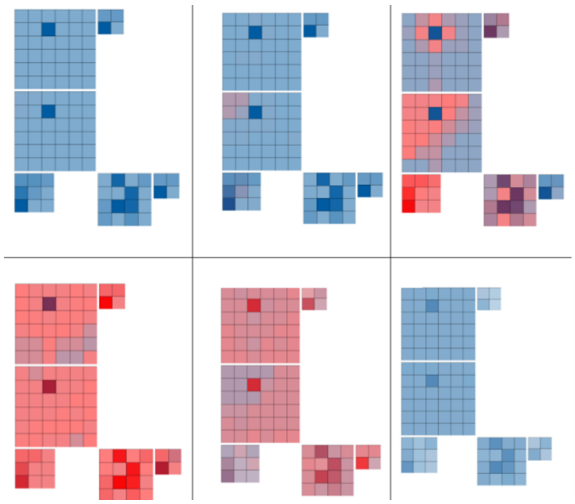

Figure 2: Example of a simulation of a disease with a 60% death rate among a fully susceptible population. The darkness/opacity of cells represents population density, and the redness represents the number in the E or I state.

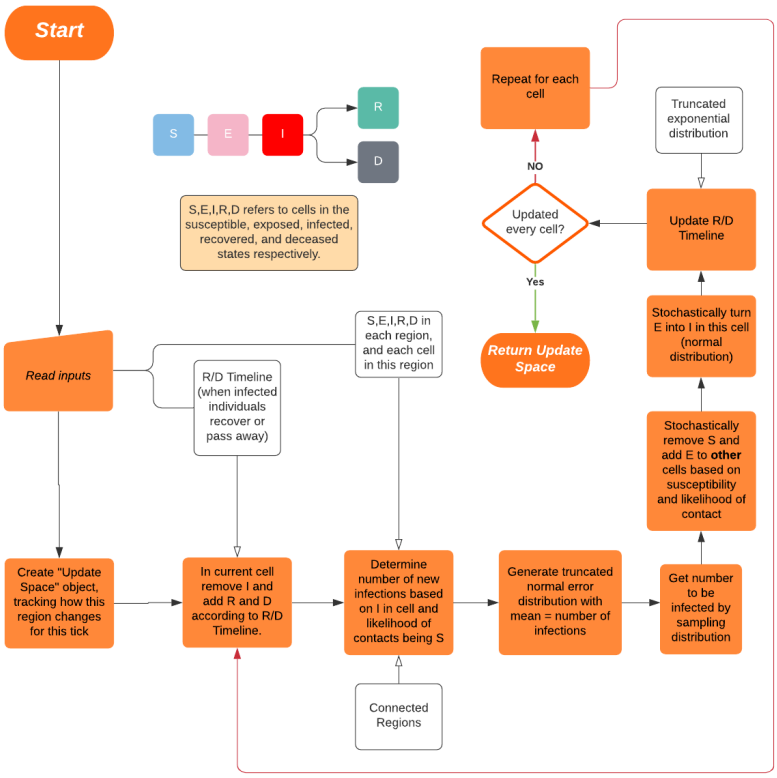

Figure 3: General process for updating a single region for one time step.

3.3.2 Faroe Islands

Measles in the Faroe Islands is chosen to be simulated since the time scale for new epidemics to appear (f^{-1}) in the Faroe Islands prior to the mass-vaccination era was approximately 590 days, much larger than the duration of epidemics, which, as discussed earlier, allows for SOC behaviour to emerge**.** Additionally, there are records dating back well before the mass-vaccination era (Rhodes, Jensen, and Anderson 1997), allowing us to consider data over a century long in this period, thus allowing us to observe the SOC behaviour.

The SOC of the islands is important, as it allows us to test our model – while it's difficult to determine the starting parameters of the Faroe Islands from a given year, the long-term irrelevance of parameters such as how many in a population are initially vulnerable should mean our model can replicate the results associated with SOC. Specifically, if our model is valid we should be able to approximate the exponent κ in the power law that epidemics in the Faroe Islands obey. From the Faroe Islands measles data, κ is estimated to be 2.265 ± 0.014 with a 95% confidence interval (Rhodes, Jensen, and Anderson 1997)

In our model, each disease-carrying individual can be considered to have a certain probability of exposing any individual within a subset of the society's population to the disease. We define C_S to be the fraction of people exposed to the disease (contacts) by the infected individual that are in the susceptible state. With R_0 being the reproduction number of the disease, the effective reproduction number for an individual will be:

$$R_e = C_S R_0 \tag{6}$$

To simulate the SOC measles epidemics of the Faroe Islands, we start by assigning a small chance each day that no individuals are infected for one at random to become infected, $f = 1/590$. Note that some "outbreaks" would disappear before being detected, as was verified when running the simulations. As such, this rate is almost certainly a lower rate than was reality. However, without knowing the likelihood of detection of small outbreaks, this is not possible to address.

We assume a population of 25,000 that starts out with 30% susceptible and 70% recovered. We also implement birth rates.[2] This is because births are a significant if not dominant source of susceptible individuals in real life, and the only source of susceptible individuals in our model. With this size population, the birth rate will be approximately constant with 1 birth a day (Rhodes, Jensen, and Anderson 1997).

Finally, we model Streymoy and Eysturoy as one large region, and we model Vágar, Sandoy, Suðuroy, and Borðoy and the surrounding small islands each as a medium region. The large region has a length 50% greater than the medium regions. See Figure 4b for an example with a medium region length of 6. We assume that each cell in each region has the same number of people.

Note that since the model is, aside from the stochastic aspects, scale invariant (since SOC cellular automata and compartmental models are scale invariant), the amount of physical area that regions represent should not be significant - but see the results section for further discussion on this.

3.3.3 Melbourne

Analysing Melbourne, we need to account for how an individual changes their behaviour in response to government measures. We define ρ to be the percentage of contacts an individual has, compared to when no pandemic is occurring. Equation (1) is now:

[2] We implement death rates too, but as a very small number of individuals other than those in the recovered state pass away, this is not significant to the results.

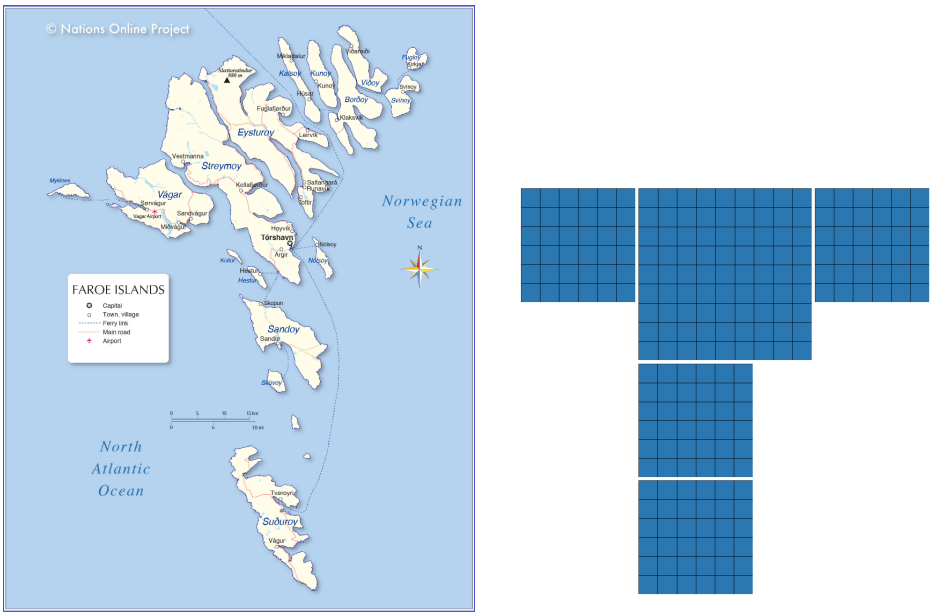

(a) **(b)**

Figure 4: (a) A map of the Faroe Islands (Source: Nations Online Project), compared with **(b)** The first frame generated by a simulation for the Faroe Islands. Each adjacent region is considered connected for this scenario.

$$R_e = \rho C_S R_0 \tag{7}$$

ρ is dependent on region, and as such allows us to model how disease spreads when lockdown measures apply differently from region to region. This idea is easily generalisable to many cases that we will not be considering - with a sufficiently sophisticated ρ function, we could model as complex and dynamic a response as we wish.

Due to the scale invariance of the model, the amount of physical area that regions represent is a matter of how granular one wants to be in modelling behavioural changes. As such, we are free to choose our regions to be the LGAs of Melbourne. For our model, we will make the simple assumption that LGAs that share a border are connected regions. If we wished, we could connect distant regions, but for our purposes this is unnecessary. Also, for this model, we only consider metropolitan Melbourne, and exclude the rural part of Victoria.

We sourced data from the Australian Bureau of Statistics to determine the size and population of each region. We assumed each cell of a region had the same population. The number of cells in each region were designated according to Table 1, such that the approximate cell size was 20 km^2. This gave the model a total of 439 cells.

LGA Area (km^2)	< 40	< 130	< 250	< 410	< 610	< 850	< 1130	$\sim$1280	$\sim$2420
Approx. LGA Area (km^2)	20	80	180	320	500	720	980	1280	2420
Cells	1	2	3	4	5	6	7	8	11

Table 1 Designation of cells to regions

The first Melbourne scenario we model is where Melbourne adopts a "blanket" lockdown strategy, where all regions adopt the same restrictions from the start of the pandemic. We assume $\rho = 0.25$. We choose $r = 0.1$ and additionally we roughly model the restrictions on movement by reducing the likelihood of interregional transmission by 95%, so that only 1/200 contacts are interregional (one can think of this as the percentage of contacts that are due to restrictions being broken, or necessary contacts across areas due to essential work).[3]

In the second scenario, we simulate what would happen if Melbourne had adopted what we will term a "reactive" lockdown implementation, as Sydney did during their outbreak. In this strategy, the restrictions of the blanket lockdown strategy only come into effect in regions/LGAs with individuals in the I state. Of course, one might object that testing and contact tracing can detect cases that are not symptomatic, which goes against the assumption here that only symptomatic cases can be detected. This is a fair point, but again, we are not aiming to accurately model the case numbers seen in Australia (and we won't), and there are other factors that could lead to infected individuals not being noticed for days while presenting symptoms.

[3]This is different to Melbourne's real movement restrictions, which instead restricted citizens to a certain distance from their homes, but implementing this detail would make it unclear whether any differences between the blanket and reactive strategies were due to the type of movement restrictions or when they were implemented. See (Kolokolnikov and Iron 2021) for how a more realistic "foraging" model for the spatial restrictions of Melbourne's strategy could be implemented.

(a)

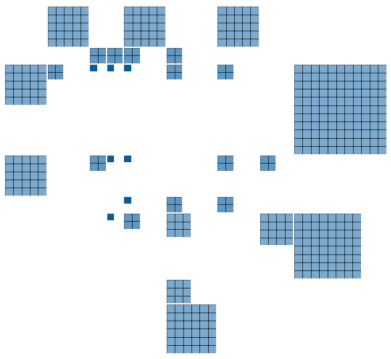

(b)

Figure 5: (a) The LGAs of metropolitan Melbourne (in blue). With the exception of Knox and Greater Dandenong, all LGAs that shared a border were considered connected (*Source: Vic Councils*). **(b)** The first frame of the simulation of Melbourne – regions are not connected by adjacency, but by the shared borders in **(a)**.

4 Results

4.1 Faroe Islands

Simulations of measles epidemics in the Faroe Islands were performed with multiple region scales. We show the largest scale used, where the large region contained 441 cells, and the medium regions each contained 196 cells.

The definition of epidemic used in Figure 6 is consecutive months where new cases were detected. For our simulation, this was done by considering a transition from the E to the I state to be a new case. The epidemic size is the number of individuals detected in this way during each epidemic. Because this method is rather granular (i.e. the incubating period for measles is less than a month), we don't need to consider the possibility that some epidemics may have been one larger epidemic with brief periods of undetected cases in between.

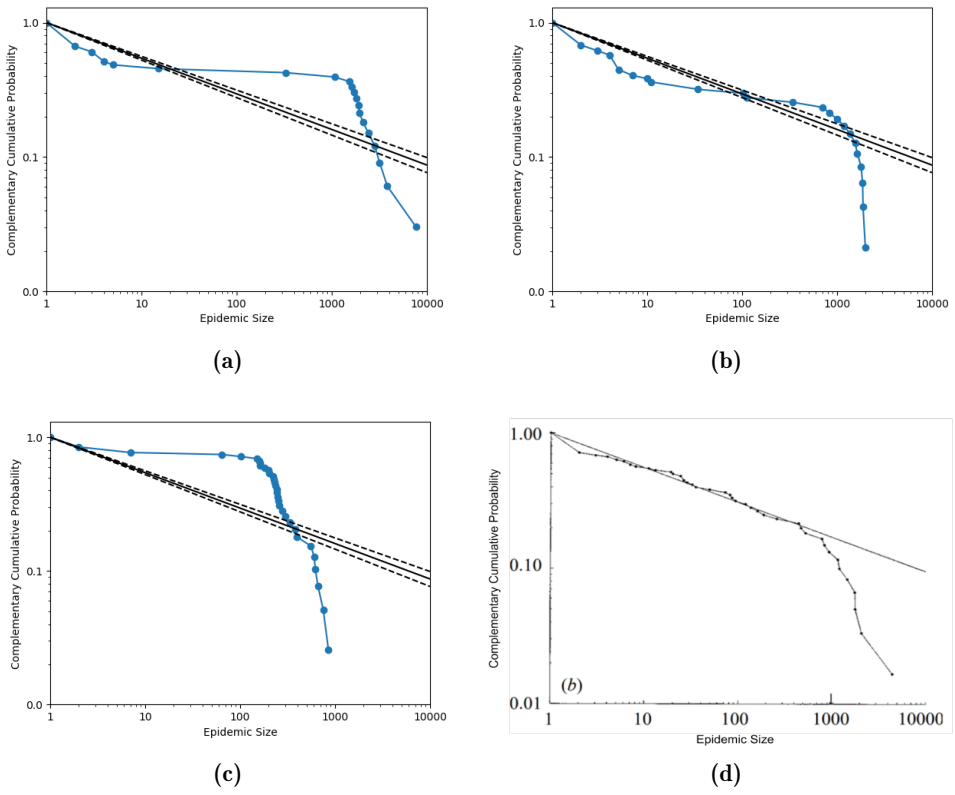

Figure 6: Plots of (complementary) cumulative probability against epidemic size taken from a 97 year simulation for regions of length 2 and 3, with **(a)** $r = 0.1$, **(b)** $r = 0.05$, and **(c)** $r = 0$. **(d)** Shows the real data for the Faroe islands over a 97 year period (from 1870 to 1970, 1866-1869 excluded). In each graph a line corresponding to a power scaling law with $\kappa = 2.265 \pm 0.014$ is shown, with the confidence interval included in **(a-c)**.

As we can see in Figure 6 (a-c), the value of r (the ratio of normal contacts to interregional contacts) has a noticeable effect on the shape of the graph. With $r = 0.005$ the plot mainly tracks the shape of the real data from the Faroe Islands, aside from there being a lower number of epidemics of size 10-800 (with slightly larger epidemics in the range above this seeming to make up for it). We believe a possible reason for this is the low number of cells exacerbating any outbreaks that gain momentum.

With more time, we could explore using a higher number of cells. The graph falls off at approximately the same point as the real data for all plots (around 1000 cases).

It's no wonder that the standard SEIR model fails to reproduce these results given the sensitivity to how frequently regional transmission occurs, and how low this is for the Faroe Islands - and we should also note our model is nowhere near perfect in modelling this. As can be seen in Figure 4a Three of the regions we have considered are connected by bridges, but two of the medium regions (the two southern Islands) are not, and thus the regional transmission rates between any two regions would not be consistent.

Finally, over a trial of 1000 years with the medium regions having 4 cells and large regions with 9, and $r = 0.05$; the average fraction of the time that the population was undergoing an epidemic was 23.72% (though this value varies little with different r values). In comparison, the real data of the Faroe Islands shows that measles was present in the population for approximately 25% of the days on record.

Interestingly, the epidemic length (in days) also closely follows a power law distribution with a similar scaling exponent value, regardless of r, and could warrant further investigation.

The model seems to be able to reproduce the SOC behaviour of epidemics in the Faroe Islands, and is able to closely follows the power law governed by the scaling exponent for measles with the right r value. Until further effort is made, it is not clear where the model breaks down (namely, in the number of medium-sized epidemics), or if the r value required to reproduce the same scaling exponent is realistic. As such, we believe it is reasonably suitable for making broad comparisons, as we will do so for the Melbourne scenario, noting that nuanced interpretations cannot be possible without knowing factors such as the (likely dynamic) r value.

4.2 Melbourne

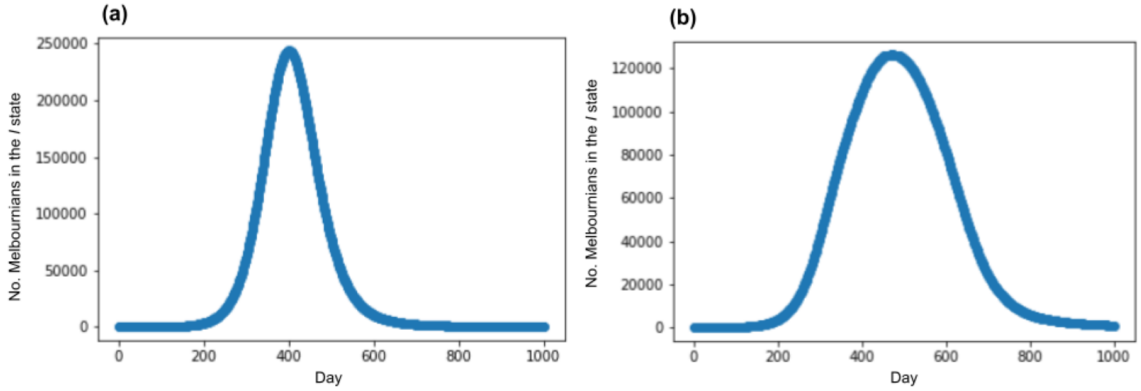

Figure 7: The number of people currently in the infected (I) state for each day of a simulation using the **(a)** reactive lockdown and **(b)** blanket lockdown.

We found that with the parameters set out in 3.3.3, the peak number of people infected was more than halved, and it took approximately 23% longer for the peak in cases to be reached.

As we would expect, the total number of cases is approximately the same for each approach, since an LGA will have the same R_e in either model as soon as an individual reaches the I state.

With harsher restrictions, the Melbourne plot becomes more irregular, as the time taken for the disease to spread to other regions grows, leading to a series of superimposed peaks.

How applicable this comparison is to reality is largely affected by the accuracy of the parameters

chosen. For example, a lower reduction in regional transmission while under restrictions leads to less of a difference between approaches. However, if the real difference is anywhere this order of magnitude, for a large outbreak the difference between the two methods could be a significant number of lives. During the initial outbreak in China, the case fatality rate was 4.5% in Wuhan, where health systems were most overwhelmed, compared to 0.5% in the rest of China, as of April 2020 – additionally, further research has supported the link between reduction in daily case numbers and lower death rates (C. 2020). Of course, there are many other things to consider in determining a response to a pandemic, and such discussion is well outside the scope of this report.

As suggested by the Faroe Islands results, a higher number of cells in the simulation could be more reliable, and since we only had 439 cells despite a population of 5 million. Unless the model is relatively scale invariant with a constant number of cells, this is a likely source of inaccuracy. With more computational power and/or time, we could use higher-cell simulations to better model the behaviour of the pandemic in Melbourne.

5 Conclusion

This report has illustrated how standard epidemiological compartmental models and SOC-behaving cellular automata can be combined and extended to produce a region-based model for epidemics. By building the model from first principles (namely, the same ideas behind the SEIR model), we demonstrated how diseases with different properties can be simulated without altering the dimensions of the cellular automaton. We then showed that the model was able to approximate the SOC behaviour of measles in the Faroe Islands prior to the mass-vaccination era, for certain modelled rates of regional transmission. Finally, we showed that this model predicts a noticeable difference between reactive and blanket lockdown strategies for an outbreak of the delta variant of COVID-19 in a large urban/metropolitan region (metropolitan Melbourne). An extension of the model through more detailed algorithms for modelling governmental response, and dynamical rather than static parameters governing contacts, could allow for more nuanced comparisons.

References

Almeida, Rodolfo Maduro, and Elbert E N Macau. 2011. "Stochastic Cellular Automata Model for Wildland Fire Spread Dynamics" 285 (March): 012038. https://doi.org/10.1088/1742-6596/285/1/012038.

Bak, Per, Chao Tang, and Kurt Wiesenfeld. 1987. "Self-Organized Criticality: An Explanation of the 1/f Noise." *Phys. Rev. Lett.* 59 (July): 381–84. https://doi.org/10.1103/PhysRevLett.59.381.

Bak, P, and M Paczuski. 1995. "Complexity, Contingency, and Criticality." *Proceedings of the National Academy of Sciences* 92 (15): 6689–96. https://doi.org/10.1073/pnas.92.15.6689.

C., Kenyon. 2020. "Flattening-the-Curve Associated with Reduced COVID-19 Case Fatality Rates- an Ecological Analysis of 65 Countries." *J Infect.* https://doi.org/doi:10.1016/j.jinf.2020.04.007.

Golyk, Vladyslav A. 2012. "Self-Organized Criticality." In.

Kalinin, N., A. Guzmán-Sáenz, Yulieth Prieto, Mikhail Shkolnikov, Vera Kalinina, and Ernesto Lupercio. 2018. "Self-Organized Criticality and Pattern Emergence Through the Lens of Tropical Geometry." *Proceedings of the National Academy of Sciences* 115 (August): 201805847. https://doi.org/10.1073/pnas.1805847115.

Kang, JaHyun, Yun Young Jang, JinHwa Kim, Si-Hyeon Han, Ki Rog Lee, Mukju Kim, and Joong Sik Eom. 2020. "South Korea's Responses to Stop the COVID-19 Pandemic." *American Journal of Infection Control* 48 (9): 1080–86. https://doi.org/https://doi.org/10.1016/j.ajic.2020.06.003.

Kolokolnikov, Theodore, and David Iron. 2021. "Law of Mass Action and Saturation in SIR Model with Application to Coronavirus Modelling." *Infectious Disease Modelling* 6: 91–97. https://doi.org/https://doi.org/10.1016/j.idm.2020.11.002.

Paul, Subhendu, and Emmanuel Lorin. 2020. "Distribution of Incubation Period of COVID-19 in the Canadian Context: Modeling and Computational Study." *medRxiv*. https://doi.org/10.1101/2020.11.20.20235648.

Pegden, W., and Annales Henri Poincaré 21 C. K. Smart. 2020. "Stability of Patterns in the Abelian Sandpile."

Rhodes, C. J., H. J. Jensen, and R. M. Anderson. 1997. "On the Critical Behaviour of Simple Epidemics." *Proceedings: Biological Sciences* 264 (1388): 1639–46. http://www.jstor.org/stable/50773.